Geometric Characteristics of Turbulent Premixed Methane-Air Flame in a Constant Volume Vessel and the Impact on Flame-Wall Interaction

Ye Wang, Shan Jiang, Mamoru Tanahashi
Department of Mechanical Engineering, Institute of Science Tokyo
2-12-1, Ookayama, Meguro-ku, Tokyo, Japan

1 Instructions

Near-wall turbulent combustion and turbulent flame-wall interaction (FWI) are widely present in combustion systems and are accompanied by near-wall flame quenching and intense wall heat flux. These phenomena are closely connected to the heat losses and operational performance of combustion devices. One of the key characteristics of turbulent flames is the unstable stretching caused by turbulence-flame interactions, leading to wrinkled flame surfaces with irregular three-dimensional geometrical structures. This topological complexity and its effects on thermochemical reactions and scalar diffusion have long been studied, primarily through flame curvature analysis, particularly mean curvature. The complex interplay between flame curvature and near-wall flame quenching during FWI has been the focus of several recent studies. Kosaka *et al.* [1] conducted experimental investigations, highlighting the flame curvature correlation with quenching behavior and heat release near the wall. Ahmed *et al.* [2] examined the topological characteristics of flame-flame interactions in turbulent boundary layers, using metrics like mean and Gaussian curvature to reveal insights into flame dynamics. Ghai *et al.* [3] explored the impact of Lewis numbers on near-wall turbulent flames, emphasizing how variations in flame curvature, reaction rates, and temperature gradients influence quenching distances and wall heat flux. Additionally, Kaddar *et al.* [4] reported a weak inversion in the relationship between flame curvature and heat release rate, suggesting a more nuanced role of curvature in FWI processes. However, it is noteworthy that in FWI, in addition to turbulence, the wall's cooling effect and physical constraints also alter the geometric properties of near-wall flames. This results in two major effects: the flame's surface geometry changes as it approaches the wall; and due to the differing physical mechanisms by which turbulence and wall effects influence flame geometry, the relationship between flame curvature and its propagation characteristics becomes more complex near the wall. To explore this complexity, the authors' previous work employed principal curvature analysis to examine the three-dimensional geometrical features of near-wall flames in a V-shaped turbulent flame in turbulent channel flow [5]. The study revealed that, compared to flames far from the wall, the combustion characteristics of near-wall turbulent flames exhibit more intricate dependencies on principal curvature, which can hardly be revealed by mean curvature analysis.

Previous research on turbulent FWI has primarily focused on open systems, particularly near-wall combustion scenarios in channel turbulence or turbulent boundary layers [2, 4–6]. However, FWI is also

Correspondence to: wang.y.by@m.titech.ac.jp

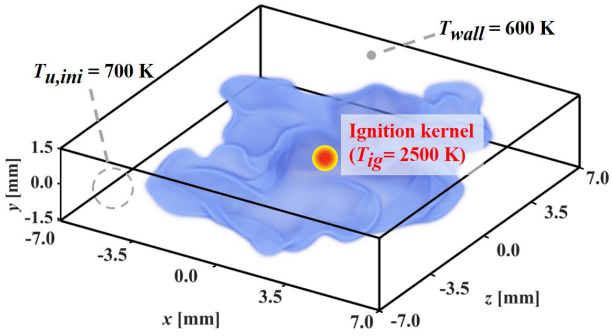

Figure 1: The geometry of the current combustion field.

prevalent in enclosed systems, such as combustion chambers in IC engines, where the flame-wall configuration differs significantly from open systems. In such case, near-wall turbulence tends to exhibit shear-free boundary layer characteristics [7]. Additionally, the overall flame geometry becomes more complex due to the influence of enclosed chamber geometry. Regarding this, the authors' previous studies used DNS of two-dimensional turbulent premixed combustion in a constant volume vessel to investigate the influence of flame-wall geometry on FWI and wall heat flux [8]. Based on these findings, a predictive model for wall heat flux during FWI was developed [9]. While, these findings require further validation in more realistic three-dimensional turbulent combustion systems. Therefore, the present study utilizes DNS data of three-dimensional turbulent premixed methane-air combustion in a constant volume vessel. Through principal curvature analysis, the study investigates the three-dimensional geometric features of near-wall flames during FWI and their influence on near-wall quenching.

2 Numerical Setups

The current DNS considers turbulent premixed methane-air combustion in a constant volume vessel. The simulation is performed using the in-house code TTX [10], which solves the fully compressible conservation equations for mass, momentum, energy, and chemical species. The temperature dependence of viscosity, thermal conductivity, and diffusion coefficients are locally calculated by CHEMKIN-II packages with modifications for combustion DNS.

The geometry of the combustion field is shown in Fig. 1. The size of the calculation domain, $l_x \times l_y \times l_z$, is $14 \times 3 \times 14$ mm^3. Non-uniform mesh is used for the numerical solution of the present DNS, where the grid size is 6.5 μm for the near-wall area and 11.6 μm for the central region. The overall resolution for each direction, $N_x \times N_y \times N_z$, is $1368 \times 322 \times 1368$. Thus, about 63 grids are within the laminar thermal flame thickness (δ^0_{th}) in the near-wall region and 35 grids in the central region under the initial condition. At the end of the whole combustion, the pressure will rise to 2.3 atmospheric pressure, and the mesh is still enough to resolve the flame structure. Iso-thermal, no-slip wall condition is set for all six boundaries of the domain with the Navier-Stokes characteristic boundary conditions (NSCBC) formulation. The wall temperature (T_{wall}) is 600 K. The methane-air mixture is set in the initial status with an equivalence ratio (ϕ) of 0.6. The preheat temperature of the mixture ($T_{u,ini}$) is 700 K, and the initial pressure (p_{ini}) is 1.0 atmospheric pressure. At the start of combustion, the fresh gas would be ignited by the high-temperature kernel imposed at the center of the domain. The CH_4 chemical mechanism used here is a reduced mechanism including 19 species and 15 lumped reaction groups out of 184 elementary reactions. A great consistency was obtained between this reduced mechanism and GRI-3.0 on transient wall heat flux, low-temperature kinetics, and other characteristics during the near-wall quenching process of premixed methane flame.

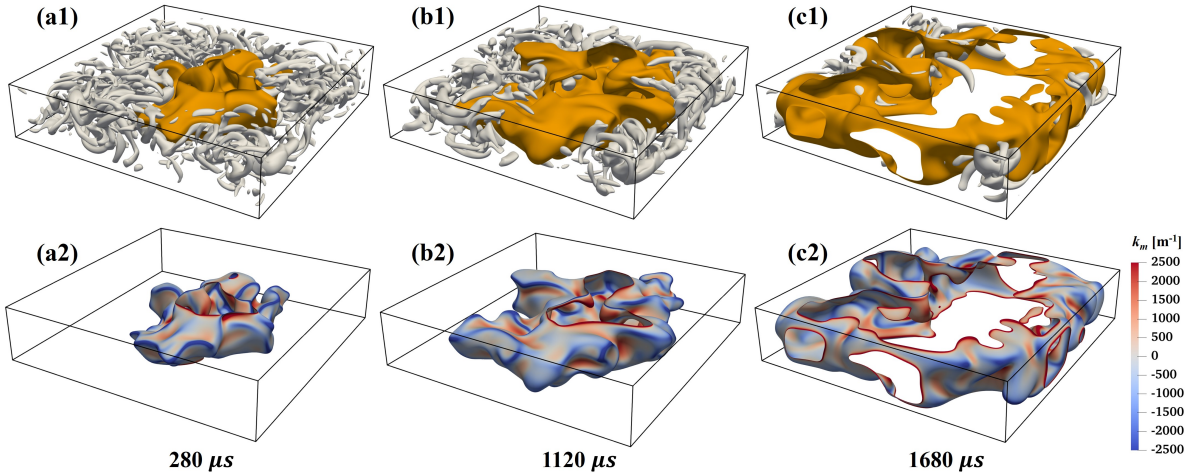

Figure 2: Instantaneous snapshots of the current combustion process (a1, b1, c1) with the orange surface representing the flame surface and gray surface representing the turbulent vortex; the flame surface color-coded by local mean curvature (a2, b2, c2).

3 Results and Discussions

3.1 Phenomenological and global characteristics

Figures 2(a1, b1, c1) depicts instantaneous snapshots of turbulent premixed methane-air combustion in a constant volume vessel. The flame surface is defined by the iso-surface of the progress variable, based on the mass fraction of CH_4, at a value of 0.7, while turbulent vortex are visualized using the Q-criterion. As can see, the flame propagates outward from the center. During this process, turbulence interacts with the flame, causing wrinkling of the flame surface. Meanwhile, due to the elongated aspect ratio of the constant volume vessel, the flame first reaches the top and bottom walls, leading to local FWI. At later stage, as shown in Figure 2 (c1), the flame reaches the side walls. Throughout this process, the flame's geometrical characteristics are influenced by both turbulence and the shape of the vessel.

The flame surface color-coded by mean curvature (k_m) is shown in Figs. 2(a2, b2, c2). In the early stages of combustion, as seen in Figs. 2(a2, b2), the flame far from the wall predominantly exhibit negative curvature, indicating that the flame is convex toward the unburned side. This occurs because the near-wall flame, experiencing flame quenching due to wall proximity, has a lower propagation speed, whereas the flame far from the wall propagates faster, leading to an overall convex shape toward the unburned side. Near the wall, turbulent vortex trapped between the flame and the wall cause a significant portion of the flame to exhibit positive curvature, convex toward the burned side. As the flame reaches the side walls, the convex geometry observed in the regions far from the walls disappears, and under the influence of near-wall turbulence, the flame becomes convex toward the burned side.

3.2 Statistical characteristics of flame geometry and its impact on flame-wall interaction

To further investigate the temporal evolution of the flame surface geometry and its changes near the wall during the combustion of turbulent premixed methane-air flames in the constant volume vessel, this study examines the principal curvatures (k_1, k_2) of the flame surface. Principal curvatures represent the maximum and minimum normal curvatures at a local point on the flame surface, and their magnitudes and relationships can be used to characterize different three-dimensional structures. Inspired by [11, 12],

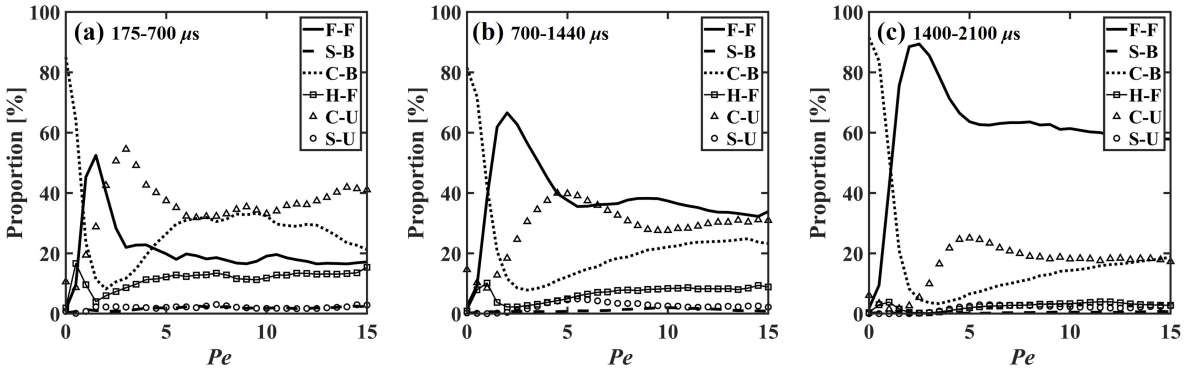

Figure 3: Proportions of flame elements with different geometric structures as functions of normalized flame-wall distance (Pe) at different combustion periods.

the flame surface is categorized into six types based on principal curvatures: (i) Flat Flame (F-F) with $\sqrt{k_1^2 + k_2^2} < 1/(\delta_{th})$; or else, (ii) Spherical flame convex to Burned side (S-B) with $k_2 > k_1/2$; (iii) Cylindrical flame convex to Burned side (C-B) with $|k_2/k_1| \leq 1/2$; (iv) Hyperbolic Flame (H-F) with $-2k_1 < k_2 < -k_1/2$; (v) Cylindrical flame convex to Unburned side (C-U) with $|k_1/k_2| \leq 1/2$; (vi) Spherical flame convex to Unburned side (S-U): $k_1 > k_2/2$.

Figure 3 shows the variation in the proportion of different geometric flame types with the flame-wall distance at different stages of combustion. Here, Pe represents the flame-wall distance normalized by the flame diffusive thickness [7]. As seen in Fig. 3(a), at the early stage of combustion and far from the wall, consistent with Fig. 2(a2), a high proportion of flames is convex toward the unburned side (e.g., C-U, S-U), accounting for over 40% at $Pe = 15$, and predominantly exhibits cylindrical shapes. As Pe decreases and the flame approaches the wall, the proportion of C-B flames increases significantly. At $Pe = 5$, the proportions of F-F and C-U flames rise. In the region where $Pe < 5$, turbulent structures dissipate under the influence of viscous effects, and the flame becomes flatter, forming a flat flame. Near the wall, differences in flame propagation speed also cause some parts of the flame to revert to being convex toward the unburned side. Due to the lack of turbulent kinetic energy input in the current constant volume vessel, unburned-side turbulence decays over time due to viscous dissipation. Accordingly, as shown in Figs. 3(b, c), the proportion of F-F flames increases over time, while the proportions of other three-dimensional flame structures decrease. However, near the wall, the same trends in flame development are observed. Additionally, in the region extremely close to the wall ($Pe < 1$), the proportion of C-B flames rises sharply. It is noteworthy that flame quenching has occurred in this region, and since the flame surface is defined based on Y_{CH_4}, the appearance of C-B structures may be attributed to the transport of CH_4 near the wall.

Figure 4 further illustrates the joint probability density function (PDF) of flame surface principal curvatures at different stages of combustion, color-coded by the normalized local fuel consumption rate (S_c/S_L). The joint PDF peaks (red line) are concentrated in the F-F region. Consistent with Figs. 2,3, during the early stages of combustion, the PDFs of flames far from the wall are concentrated in the convex-to-unburned-side region, predominantly in the C-U category. As combustion progresses, the PDF values in the high-curvature C-U region decrease, while those in the high-curvature C-B region increase, indicating a shift toward convex-to-burned-side structures at later stages. This temporal evolution of PDF distribution is not observed in our previous steady-state DNS [5]. Near the wall, the joint PDF of flame principal curvatures is more concentrated in the C-U and C-B regions, corresponding to cylindrical flames convex to either the burned or unburned side.

In terms of local fuel consumption rate, flames far from the wall exhibit higher S_c/S_L in the convex-to-

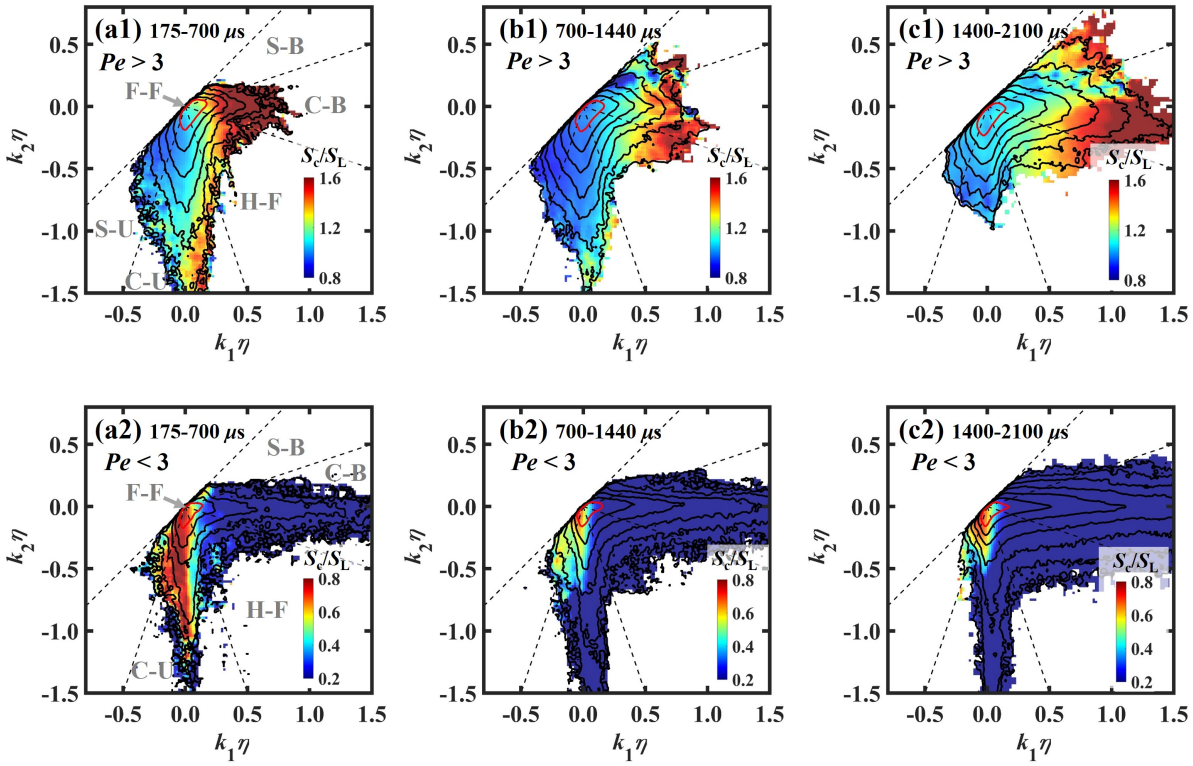

Figure 4: Contours of joint probability density function between flame's principal curvatures (k_1, k_2) with different ranges of flame-wall distance and mean values of normalized fuel consumption speed (S_c/S_L).

burned-side region. Overall, S_c/S_L shows a positive correlation with curvature, meaning flames convex to the burned side are more reactive. Near the wall, due to quenching, the local S_c/S_L decreases compared to flames farther from the wall. Unlike far-wall flames, relatively high S_c/S_L values are observed on the convex-to-unburned-side flames near the wall. This indicates a change in the dependence of S_c/S_L on curvature as the flame approaches the wall, which has been reported in the authors' previous study [5] with significantly impacts on FWI characteristics.

4 Conclusions

This study investigates the three-dimensional geometric characteristics of turbulent premixed methane-air flame in a constant volume vessel and their impact on FWI using DNS. The findings reveal that, under the combined influence of turbulence and wall constraints, the flame undergoes a temporal transition from being predominantly convex to the unburned side to convex to the burned side during combustion. Additionally, the relationship between flame curvature and reactivity changes as the flame approaches the wall, further influencing near-wall quenching behavior.

References

[1] H. Kosaka, F. Zentgraf, A. Scholtissek, C. Hasse, and A. Dreizler, "Effect of Flame-Wall Interaction on Local Heat Release of Methane and DME Combustion in a Side-Wall Quenching Geometry," *Flow Turbul. Combust.*, vol. 104, no. 4, pp. 1029–1046, 2020.

[2] U. Ahmed, S. P. Malkeson, A. L. Pillai, N. Chakraborty, and R. Kurose, "Flame self-interaction during turbulent boundary layer flashback of hydrogen-rich premixed combustion," *Physical Review Fluids*, vol. 8, no. 2, pp. 1–15, 2023.

[3] S. K. Ghai, U. Ahmed, and N. Chakraborty, "Effects of Fuel Lewis Number on Wall Heat Transfer During Oblique Flame-Wall Interaction of Premixed Flames Within Turbulent Boundary Layers," *Flow, Turbulence and Combustion*, vol. 111, no. 3, pp. 867–895, 2023.

[4] D. Kaddar, M. Steinhausen, T. Zirwes, H. Bockhorn, C. Hasse, and F. Ferraro, "Combined effects of heat loss and curvature on turbulent flame-wall interaction in a premixed dimethyl ether/air flame," *Proc. Combust. Inst.*, vol. 39, no. 2, pp. 2199–2208, 2023.

[5] Y. Wang and M. Tanahashi, "Three-dimensional geometrical effects on the near-wall quenching of turbulent premixed flame," *Proceedings of the Combustion Institute*, vol. 40, no. 1-4, p. 105629, 2024.

[6] A. Gruber, R. Sankaran, E. R. Hawkes, and J. H. Chen, "Turbulent flame-wall interaction: A direct numerical simulation study," *J. Fluid Mech.*, vol. 658, pp. 5–32, 2010.

[7] T. J. Poinsot, D. C. Haworth, and G. Bruneaux, "Direct simulation and modeling of flame-wall interaction for premixed turbulent combustion," *Combust. Flame*, vol. 95, no. 1-2, pp. 118–132, 1993.

[8] Y. Wang, Y. Minamoto, M. Shimura, and M. Tanahashi, "Quenching modes of local flame–wall interaction for turbulent premixed methane combustion in a constant volume vessel," *Combustion Theory and Modelling*, vol. 27, no. 6, pp. 715–735, 2023.

[9] T. Kaminaga, Y. Wang, and M. Tanahashi, "Modeling of wall heat flux in flame–wall interaction using machine learning," *International Journal of Heat and Fluid Flow*, vol. 112, no. December 2024, p. 109727, 2025.

[10] M. Tanahashi, M. Fujimura, and T. Miyauchi, "Coherent fine-scale eddies in turbulent premixed flames," *Proc. Combust. Inst.*, vol. 28, no. 1, pp. 529–535, 2000.

[11] Y. Shim, S. Tanaka, M. Tanahashi, and T. Miyauchi, "Local structure and fractal characteristics of H2-air turbulent premixed flame," *Proc. Combust. Inst.*, vol. 33, no. 1, pp. 1455–1462, 2011.

[12] T. L. Howarth, E. F. Hunt, and A. J. Aspden, "Thermodiffusively-unstable lean premixed hydrogen flames: Phenomenology, empirical modelling, and thermal leading points," *Combust. Flame*, vol. 253, p. 112811, 2023.